Eur. J. Mech., B/Fluids, **17**, n° 2, 205-217, 1998

Oblique two-fluid stagnation-point flow

B. S. TILLEY *, [1] **and P. D. WEIDMAN** *, [2]

ABSTRACT. – Exact similarity solutions for the impingement of two viscous, immiscible oblique stagnation flows forming a flat interface are given. The problem is governed by three parameters: the ratios of density $\rho = \rho_1/\rho_2$ and of viscosity $\mu = \mu_1/\mu_2$ of the two fluids and $R = \tan\theta_1/\tan\theta_2$ where θ_1 and θ_2 are the asymptotic angles of the incident streamlines in each fluid layer. For given values of ρ, μ, and θ_2, the compatible flows in the lower fluid, as measured by the strain rate ratio $\beta = \beta_1/\beta_2$ of the two fluids and the asymptotic angle of incidence θ_1, are found such that the interface remains horizontal in a uniform gravitational field. For $\rho = 1$, explicit solutions show that a family of co-current and counter-current shears supporting a flat interface exist for all finite, nonzero values of R. For $\rho \neq 1$, the normal stress interfacial boundary conditions restricts the flow to a unique combination of asymptotic far-field shear and Hiemenz stagnation-point flow in each fluid layer. The displacement thicknesses in each layer are always positive when the fluid densities are not equal, but vanish simultaneously as $\rho \to 1$. At each value of ρ the interfacial velocities increase with increasing viscosity ratio μ. As a generalization of the present oblique two-fluid stagnation-point flow problem, we discuss how the flat interface may be inclined with respect to the horizontal in a uniform gravitational field. © Elsevier, Paris.

1. Introduction

Stagnation-point flows are ubiquitous in the sense that they inevitably appear as a component of more complicated flow fields. In some situations flow is stagnated by a solid wall, while in others there is a free stagnation point or line interior to a homogeneous fluid domain, or at the interface between two immiscible fluids. These can be either viscous or inviscid, steady or unsteady, two-dimensional or three-dimensional, normal or oblique, and forward or reverse. The classic problems of two-dimensional and axisymmetric three-dimensional stagnation-point flow are associated with the names (Hiemenz, 1911) and (Homann, 1936), respectively. Forward and reverse two-fluid stagnation-point flows occur naturally, for example, at the front and rear of a liquid sphere of one fluid in uniform translation through a quiescent immiscible fluid of a different kind, a problem solved in the low Reynolds number limit by (Hadamard, 1911). Generalized three-dimensional stagnation-point flow, composed of the nonlinear interaction between two orthogonal Hiemenz flows of arbitrary strain rate, was reported by (Howarth, 1951). Reverse stagnation-point flow against an impermeable flat wall does not exist in two dimensions, but (Davey, 1960) showed that certain reverse flows in three dimensions are possible. A novel radial stagnation flow impinging axisymmetrically on a circular cylinder was reported by (Wang, 1974). Of interest in the present study is oblique stagnation-point flow. (Stuart, 1959) first gave the solution for planar oblique stagnation-point flow impinging on a flat plate, a result later rediscovered by (Tamada, 1979) and (Dorrepaal, 1985). Unsteady stagnation-point flows abound, and an interesting solution was found recently by (Burdé, 1996) that corresponds to reverse stagnation flow with time-dependent blowing through a flat porous surface. The pervasive feature of the stagnation flows cited above is that they all represent exact solutions of the Navier-Stokes equations.

* Laboratoire d'Hydrodynamique (LadHyX), École Polytechnique, F-91128 Palaiseau Cedex, France.
[1] Permanent address: Department of Mathematical Sciences, New Jersey Institute of Technology, University Heights, Newark, NJ 07102 USA.
[2] Permanent address: Department of Mechanical Engineering, University of Colorado, Boulder, CO 80309 USA

0997-7546/98/02/© Elsevier, Paris

Two papers by C. Y. Wang bear on the present study. In the first (Wang, 1985) considered the normal stagnation-point flow of one fluid on a quiescent second fluid. Implicit in that paper is the assumption that the normal-stress boundary condition at the two-fluid interface is satisfied approximately, by virtue of the fact that the two-fluid density ratio is large, or that the solution is valid only in a small neighborhood of the flat interface around the stagnation point. In the second paper (Wang, 1992) solved for the spatially-developing boundary layers produced by uniform shear flow of one fluid (*eg.* air) over a second quiescent fluid (*eg.* water). The two-fluid oblique stagnation flow considered here combines certain aspects of both these problems. In another two-fluid flow study, (Coward and Hall, 1996) considered the class of flows whereby an upper stagnation-point flow of one fluid (*eg.* gas) impinges normally on a uniform depth liquid layer (*eg.* liquid) undergoing blowing or suction at its lower boundary. Intended as a model of air flow over flow over a swept wing covered by a thin layer of water, they found unique steady solutions dependent on the strength of blowing or suction in the lower liquid layer. The stability of that two-fluid system to transverse periodic pertubations was analyzed. In the current problem, there is no equivalent to the suction/blowing flows due to the lack of a lower boundary, but it would be interesting, and perhaps more realistic from an application point of view, to generalize the (Coward and Hall, 1996) problem by considering an oblique stagnation-point flow of the gas.

Our paper is organized as follows. The two-fluid similarity formulation is given in §2. Explicit solutions for equally dense fluids are given in §3. Numerical solutions of the governing ordinary differential equations covering a comprehensive range of density and viscosity ratios are presented in §4, and concluding remarks are given in §5.

2. Problem formulation

Consider a liquid of density ρ_1 and viscosity μ_1 in static equilibrium beneath a second immiscible fluid of density ρ_2 and viscosity μ_2 in a uniform gravitational field g. The far-field stagnation flow is characterized by strain rate β_2 and streamline angle θ_2 and we take, without loss of generality, $0 < \theta_2 \leq \pi/2$. When velocity fields $\mathbf{u}^{(1)}$ and $\mathbf{u}^{(2)}$ are nonzero the flow of each fluid is assumed to be incompressible. Scaling coordinates with $\sqrt{\mu_2/\rho_2\beta_2}$, time with $1/\beta_2$, velocites with $\sqrt{\mu_2\beta_2/\rho_2}$, and pressures with $\mu_2\beta_2$, the continuity and Navier-Stokes equations in each fluid are given by

$$\boldsymbol{\nabla} \cdot \mathbf{u}^{(1)} = 0 \tag{1}$$

$$\frac{D\mathbf{u}^{(1)}}{Dt} = -\frac{1}{\rho}\boldsymbol{\nabla} p^{(1)} + \frac{\mu}{\rho}\nabla^2 \mathbf{u}^{(1)} \tag{2}$$

$$\boldsymbol{\nabla} \cdot \mathbf{u}^{(2)} = 0 \tag{3}$$

$$\frac{D\mathbf{u}^{(2)}}{Dt} = -\boldsymbol{\nabla} p^{(2)} + \nabla^2 \mathbf{u}^{(2)} \tag{4}$$

where $\rho = \rho_1/\rho_2$ is the density ratio, $\mu = \mu_1/\mu_2$ is the viscosity ratio, and $p^{(i)}$, $i = 1, 2$, are the reduced pressures that take into account the different uniform static pressure gradients in each fluid. The Cartesian coordinates for the planar problem are (x, z) and the uniform gravitational field points along negative z. For static equilibrium, $\rho > 1$. We seek the compatible oblique stagnation-point flow of the lower fluid, characterized by strain rate β_1 and the asymptotic streamline angle $0 < \theta_1 < \pi$. Since the strain rate β_2 of the upper fluid has been scaled out of the problem, the input parameters are ρ, μ, and θ_2. A typical two-fluid solution showing the Cartesian coordinates and our reference system defining the asymptotic stagnation angles θ_1 and θ_2 is given in Figure 1.

It is convenient to introduce a streamfunction satisfying continuity equations (1) and (3) in each fluid according to

$$\mathbf{u}^{(i)} = -\boldsymbol{\nabla} \wedge \left[\psi^{(i)}(x, z)\mathbf{j}\right].$$

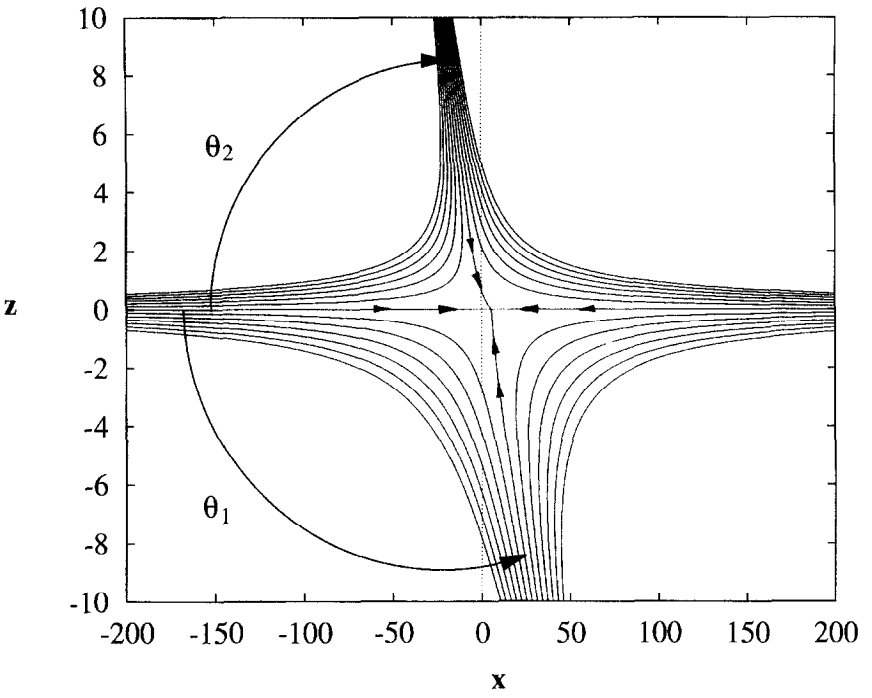

Fig. 1. – Oblique two-fluid stagnation flow streamline field for $\mu = 10$, $\rho = 15$ and $\theta_2 = 72.2^o$. The solution for the lower fluid response gives $\theta_1 = 115.2^o$ and $\beta = 0.223$. Also displayed are the Cartesian coordinate system and our definitions for θ_1 and θ_2. Note the difference in scales between the horizontal and vertical directions which distort the asymptotic streamline angles.

As shown by (Stuart, 1959), the rotational far-field motion for oblique stagnation-point flow is a linear superposition of uniform shear and Hiemenz flow. Following (Dorrepaal, 1985) we parameterize the relative strengths of these far-field flows in each fluid layer according to

$$\psi_z^{(1)} \sim \beta(x \sin\alpha_1 - z\cos\alpha_1) \qquad (z \to -\infty) \tag{5}$$

$$\psi_z^{(2)} \sim x \sin\alpha_2 + z\cos\alpha_2 \qquad (z \to +\infty). \tag{6}$$

It must be emphasized that the angles α_1 and α_2 are simply parameters that provide a continuous transition from Hiemenz stagnation-point flows at $\alpha_i = \pi/2$ to continuous or discontinuous uniform shear flows at $\alpha_i = 0$, $i = 1, 2$ for the inviscid problem. By the convention shown in Figure 1 the actual asymptotic angles of the impinging flows are given by

$$\theta_i = \tan^{-1}(2\tan\alpha_i) \qquad (i = 1, 2). \tag{7}$$

The boundary conditions at the horizontal interface we locate at $z = 0$ are continuity of streamfunction, tangential velocity, and horizontal and normal stresses which, applied in that order, are given by

$$\psi^{(2)} - \psi^{(1)} = 0, \quad \psi_z^{(2)} - \psi_z^{(1)} = 0, \quad \psi_{zz}^{(2)} - \mu\psi_{zz}^{(1)} = 0 \tag{8}$$

$$p^{(1)} - p^{(2)} + 2\left[\mu\psi_{xz}^{(1)} - \psi_{xz}^{(2)}\right] = 0. \tag{9}$$

Inserting similarity solution forms

$$\psi^{(i)}(x, z) = x f_i(z) + g_i(z) \tag{10}$$

into the far-field conditions (5) and (6) yields

$$f_1'(-\infty) = \beta \sin\alpha_1, \qquad g_1''(-\infty) = -\beta\cos\alpha_1 \tag{11}$$

$$f_2'(\infty) = \sin\alpha_2, \qquad g_2''(\infty) = \cos\alpha_2 \tag{12}$$

where a prime denotes differentiation with respect to z. Inserting (10) into momentum equations (2) and (4) furnishes a system of homogeneous partial differential equations which may be integrated once with respect to z. Evaluation of those equations in the far-field using (11) and (12) then yields

$$\frac{\mu}{\rho} f_1''' + f_1 f_1'' - (f_1')^2 = -\beta^2 \sin^2\alpha_1 \tag{13}$$

$$\frac{\mu}{\rho} g_1''' + g_1'' f_1 - g_1' f_1' = \beta K_1 \cos\alpha_1 \tag{14}$$

$$f_2''' + f_2 f_2'' - (f_2')^2 = -\sin^2\alpha_2 \tag{15}$$

$$g_2''' + g_2'' f_2 - g_2' f_2' = -K_2 \cos\alpha_2, \tag{16}$$

where K_1 and K_2, to be determined numerically, are related to the constant dimensional displacement thicknesses δ_i^* in each fluid through the relations

$$\delta_1^* = \sqrt{\frac{\nu_2}{\beta_2}}\,\rho^{1/2}\,\frac{K_1}{\sin\alpha_2}; \qquad \delta_2^* = \sqrt{\frac{\nu_2}{\beta_2}}\,\frac{K_2}{\sin\alpha_2}. \tag{17}$$

Also, f_1 and f_2 satisfy the far-field relations

$$f_1(z) \sim \beta z \sin\alpha_1 - K_1 \qquad (z \to -\infty) \tag{18}$$

$$f_2(z) \sim z \sin\alpha_2 - K_2 \qquad (z \to +\infty). \tag{19}$$

After determining the primary flow solutions $f_1(z)$ and $f_2(z)$, the pressure fields in each fluid may be calculated from the equation

$$p^{(i)}(x,z) = -\frac{\mu_i}{\mu_2} f_i' - \frac{\rho_i}{\rho_2}\left[\frac{1}{2} f_i^2 + (-1)^i \frac{\beta_i}{\beta_2} K_i\, x \cos\alpha_i + \frac{x^2}{2}\left(\frac{\beta_i}{\beta_2}\sin\alpha_i\right)^2\right] + P_i,$$

where the P_i are constant reference pressures. Application of the normal stress condition (9) gives the following three results

$$\beta = \frac{1}{\sqrt{\rho}}\frac{\sin\alpha_2}{\sin\alpha_1}, \qquad K_2 \tan\alpha_1 = -\sqrt{\rho} K_1 \tan\alpha_2, \qquad P_2 = P_1 + (\mu - 1) f_2'(0). \tag{20}$$

Thus the far-field structure of the flow in the lower fluid, governed by β_1 and α_1 (through which one obtains θ_1), is completely determined by matched solutions of equations (13) and (15); then equations (14) and (16) are solved to smoothly connect the uniform far-field shear components across the interface.

Canonical Hiemenz equations in each fluid may be obtained using the affine transformations

$$f_1(z) = \frac{\mu}{\rho} s_1 F_1(s_1 z), \qquad g_1'(z) = -\frac{\beta}{s_1} H_1(s_1 z)\cos\alpha_1 \tag{21}$$

$$f_2(z) = s_2 F_2(s_2 z), \qquad g_2'(z) = \frac{1}{s_2} H_2(s_2 z)\cos\alpha_2 \tag{22}$$

where $s_1 = -\rho^{1/4}\mu^{-1/2}\sqrt{\sin\alpha_2}$ and $s_2 = \sqrt{\sin\alpha_2}$. Then equations (13)-(16) become

$$F_1''' + F_1F_1'' - (F_1')^2 = -1, \quad F_2''' + F_2F_2'' - (F_2')^2 = -1, \tag{23}$$

$$H_1'' + F_1H_1' - F_1'H_1 = A_1, \quad H_2'' + F_2H_2' - F_2'H_2 = -A_2, \tag{24}$$

with $A_1 = \rho^{3/4}\mu^{-1/2}K_1/\sqrt{\sin\alpha_2}$ and $A_2 = K_2/\sqrt{\sin\alpha_2}$. The selections $s_1 < 0$ and $s_2 > 0$ gives a positive independent variable ζ in each layer defined by

$$\zeta = \begin{cases} s_1 z, & z \le 0 \\ s_2 z, & z \ge 0 \end{cases} \tag{25}$$

introduced to facilitate the numerical integrations. The far-field boundary conditions are now

$$F_1'(\infty) = H_1'(\infty) = F_2'(\infty) = H_2'(\infty) = 1, \tag{26}$$

and the interfacial conditions are given by

$$F_1(0) = F_2(0) = 0, \qquad \rho^{1/2}F_2'(0) - F_1'(0) = 0, \qquad \rho^{1/4}F_2''(0) + \mu^{1/2}F_1''(0) = 0 \tag{27}$$

$$\rho^{1/2}H_2(0) + \frac{A_2}{A_1}H_1(0) = 0, \qquad \rho^{1/4}H_2'(0) - \mu^{1/2}\frac{A_2}{A_1}H_1'(0) = 0. \tag{28}$$

Finally, α_1 may be calculated from $(20)_2$ which now reads

$$\tan\alpha_1 = -\frac{\mu^{1/2}}{\rho^{1/4}}\frac{A_1}{A_2}\tan\alpha_2 \tag{29}$$

wherein

$$A_1 = \lim_{\zeta\to\infty}\{F_1(\zeta) - \zeta\}, \qquad A_2 = \lim_{\zeta\to\infty}\{\zeta - F_2(\zeta)\}. \tag{30}$$

In §§3 and 4 the factors A_1 and A_2, proportional to the displacement thickness in each fluid layer, are found to be positive, as expected. Thus α_1, and therefore θ_1 calculated from equation (7), both fall in the range $[0, \pi]$.

3. The case $\rho = 1$

Explicit solutions may be found for equally dense fluids in each layer. By inspection, $F_1 = F_2 = \zeta$ are exact solutions satisfying the normalized Hiemenz equations and all associated boundary conditions. This represents the normal impingement of two, equal-strength, potential stagnation-point flows for which $K_1 = K_2 = 0$ and hence equation $(20)_2$ is satisfied identically. Note that equation $(20)_1$ then yields a one-parameter definition for β in terms of α_1, for fixed α_2 with $\rho = 1$. The H_i satisfy the identical second-order equations

$$H_i'' + \zeta H_i' - H_i = 0 \tag{31}$$

with interfacial and far-field boundary conditons given by

$$R\,H_2(0) - \sqrt{\mu}\,H_1(0) = 0, \qquad R\,H_2'(0) + \mu\,H_1'(0) = 0 \tag{32}$$

$$H_i'(\zeta) \to 1, \qquad \text{as } \zeta \to \infty, \tag{33}$$

where we have introduced $R = \tan\alpha_1/\tan\alpha_2$. By inspection $H_i = \zeta$ is one solution of (31) and the second homogeneous solution may be found by standard techniques leading to the general solution

$$H_i(\zeta) = C_i\,\zeta + D_i\left[e^{-\zeta^2/2} + \sqrt{\frac{\pi}{2}}\,\zeta\,\mathrm{erf}\left(\frac{\zeta}{\sqrt{2}}\right)\right]. \tag{34}$$

Boundary conditions (32) and (33) form a linear system determining the unknown constants C_i and D_i, with solution

$$C_1 = \frac{\sqrt{\mu} - R}{\sqrt{\mu}(\sqrt{\mu}+1)}, \qquad D_1 = \sqrt{\frac{2}{\pi}}\,\frac{\mu + R}{\sqrt{\mu}(\sqrt{\mu}+1)} \tag{35}$$

$$C_2 = \sqrt{\mu}\,\frac{R - \sqrt{\mu}}{R(1+\sqrt{\mu})}, \qquad D_2 = \sqrt{\frac{2}{\pi}}\,\frac{\mu + R}{R(\sqrt{\mu}+1)}. \tag{36}$$

A final integration of (34) provides the full solution, written here in the original variable z as

$$f_1(z) = f_2(z) = z\,\sin\alpha_2 \tag{37}$$

$$g_1(z) = -\mu\cot\alpha_1\left\{C_1\frac{\sin\alpha_2}{2\mu}\,z^2 + D_1\sqrt{\frac{\pi}{2}}\left[\left(1 + \frac{\sin\alpha_2}{2\mu}\,z^2\right)\mathrm{erf}\left(\sqrt{\frac{\sin\alpha_2}{2\mu}}\,z\right) - \frac{1}{\sqrt{\pi}}\gamma\left(\frac{3}{2}, \frac{\sin\alpha_2}{2\mu}\,z^2\right)\right]\right\} \tag{38}$$

$$g_2(z) = \frac{\cos\alpha_2}{\sin\alpha_1}\left\{C_2\frac{\sin\alpha_2}{2}\,z^2 + D_2\sqrt{\frac{\pi}{2}}\left[\left(1 + \frac{\sin\alpha_2}{2}\,z^2\right)\mathrm{erf}\left(\sqrt{\frac{\sin\alpha_2}{2}}\,z\right) - \frac{1}{\sqrt{\pi}}\gamma\left(\frac{3}{2}, \frac{\sin\alpha_2}{2}\,z^2\right)\right]\right\}, \tag{39}$$

in which $\gamma(q,z)$ is the incomplete gamma function of parameter q and variable z as defined in (Abramowitz and Stegun, 1972). The horizontal interfacial velocity $u(x,0)$, calculated with the aid of (34), and the position $(x_0,0)$ of the stagnation point are readily determined to be

$$u(x,0) = \sqrt{\frac{2}{\pi}}\,\frac{\mu + R}{R(\sqrt{\mu}+1)}\,\frac{\cos\alpha_2}{\sqrt{\sin\alpha_2}} + x\sin\alpha_2, \qquad x_0 = -\sqrt{\frac{2}{\pi}}\,\frac{\mu + R}{R(\sqrt{\mu}+1)}\,\frac{\cos\alpha_2}{(\sin\alpha_2)^{3/2}}. \tag{40}$$

A sample solution for $\mu = 5$ and $R = 0.5$ is given in Figure 2. There is a turning point along the separating streamline in the upper fluid that extends horizontally beyond the stagnation point. This point coincides with the minimum (maximum) horizontal fluid velocity for values of x greater than (less than) zero. Figure 2 also exhibits horizontal velocity profiles at positions $x = x_0$, $x = x_0 \pm 5$ and $x = x_0 \pm 15$, symmetrically distributed about the stagnation point. Although the shape of the curves are x-independent, the velocity profiles at the different spatial locations are markedly different, with flow reversal occuring near to, and upstream of, the stagnation point.

Topological characteristics of the flow may be understood through a determination of the streamline slopes at the stagnation point. We first calculate the slope dz/dx along an arbitrary streamline. Values of the streamline slopes at the stagnation point $(x_0,0)$, along with knowledge of the oblique stagnation flow angles θ_1 and θ_2, can be used to determine the existence of turning points (dz/dx infinite) along the separating streamlines in each fluid layer. Setting $x = x_0$ in the expression for dz/dx and taking the limit $z \to 0$, using L'Hospital's rule, furnishes the stagnation-point slopes

$$m_1 \equiv \left(\frac{dz}{dx}\right)_{(x_0,0^-)} = \frac{(1+\sqrt{\mu})R}{\sqrt{\mu}(\sqrt{\mu} - R)}\tan\alpha_2, \qquad m_2 \equiv \left(\frac{dz}{dx}\right)_{(x_0,0^+)} = \frac{\mu(1+\sqrt{\mu})R}{(\sqrt{\mu} - R)}\tan\alpha_2. \tag{41}$$

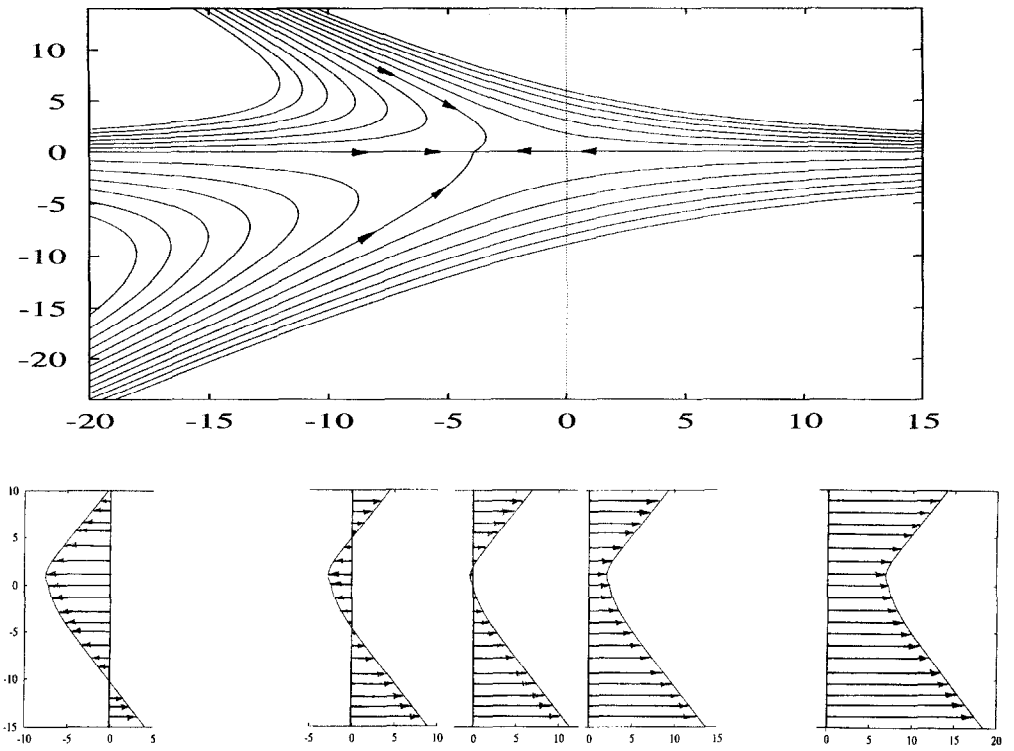

Fig. 2. – Streamline field given by the equal density explicit solution $\mu = 5$, $R = 0.5$, and $\theta_2 = \theta_2 = 28.65^{\circ}$. Note the turning point where the separating stagnation streamline is at an extremum in x. Below are the horizontal velocity profiles at axial positions $x = x_0$, $x = x_0 \pm 5$ and $x = x_0 \pm 15$, where $x_0 = -3.91$.

The following observations may now be made. Firstly, the streamline slopes at the stagnation point in each fluid are of the same sign, regardless of the values of μ and R. Secondly, $|m_1| < |m_2|$ for $\mu < 1$, $|m_1| > |m_2|$ for $\mu > 1$, and the ratio of the magnitude of the slopes is $|m_1/m_2| = \mu^{3/2}$. Thirdly, the slopes at the interface are continuous only when $\mu = 1$. The location of the stagnation point $(x_0, 0)$ at the interface and the nature of possible turning points depends on the sign of R. Consider $R > 0$ in which case $x_0 < 0$ always according to $(40)_2$. Then for $\mu^{1/2} > R$ one has $m_1 > m_2 > 0$ when $0 < \mu < 1$, or $0 < m_1 < m_2$ when $1 < \mu < \infty$, and a turning point in the stagnation streamline must exist in the upper fluid layer in order that the streamline match its negative slope in the far field as $z \to \infty$. For $\mu^{1/2} < R$, on the other hand, one has $m_2 < m_1 < 0$ when $0 < \mu < 1$, or $m_1 < m_2 < 0$ when $1 < \mu < \infty$, and a turning point on the stagnation streamline appears in the lower fluid. In the special case $\mu^{1/2} = R \neq 1$, the stagnation streamlines in each fluid join smoothly with infinite slope at the interface, but the flow possesses no symmetry: only for identical fluids for which $R = 1$ is the flow symmetric about the interface. Next consider $R < 0$ in which case the stagnation-point streamline slopes in each layer are always negative and no turning points exist anywhere. In this circumstance the horizontal position of the stagnation point may be positive or negative. In particular, $x_0 < 0$ for $\mu > |R|$, $x_0 > 0$ for $\mu < |R|$, and the stagnation point is precisely at the origin whenever $\mu = |R|$. The above results are summarized in Table 1.

4. Numerical solutions

For $\rho \neq 1$ the coupled system of equations (23) and (24) are solved numerically, shooting with a fourth order Runge-Kutta integration routine embedded in a Newton-Raphson method for ascertaining subsequent estimates of unknown interfacial velocity and shear stress parameters. The Hiemenz equations (23) are solved first to

TABLE I. – Topology of the turning point of the stagnation streamline and the relative location of the stagnation point for $\rho = 1$. Note that $\mu^{1/2} = R$ corresponds to the case when the stagnation point is the turning point.

<table>
<tr><td colspan="2">$R > 0$</td><td colspan="2">$R < 0$</td></tr>
<tr><td>$\mu^{1/2} < R$</td><td>Turning Point in Upper Layer</td><td colspan="2" rowspan="2">No Stagnation Streamline Turning Points</td></tr>
<tr><td>$\mu^{1/2} > R$</td><td>Turning Point in Lower Layer</td></tr>
<tr><td colspan="2" rowspan="2">$x_0 < 0$ Always</td><td>$\mu > R$</td><td>$x_0 < 0$</td></tr>
<tr><td>$\mu < R$</td><td>$x_0 > 0$</td></tr>
</table>

determine, *inter alia*, the constants A_i from (30). Subsequently, the coupled system (23) and (24) are integrated simultaneously, iterating only on the unknown parameters in the interfacial conditions (28) determining H_i. In Newton's method, an iteration is made on the coefficients S_i and T_i in the asymptotic behaviors

$$F_i \sim \eta_i - S_i \frac{1}{\eta_i^4} e^{-\eta_i^2/2} \tag{42}$$

$$H_i \sim \eta_i + (-1)^i A_i - T_i e^{-\eta_i^2/2}, \tag{43}$$

where $\eta_i = \zeta - (-1)^i A_i$, until the interfacial conditions are satisfied to prescribed accuracy. In the following only statically-stable stratifications ($\rho > 1$) are considered.

Figure 3 exhibits the displacement thicknesses K_i as a function of $1/\rho$ at selected values of μ. (Davey, 1960) has shown that the displacement thickness in certain three dimensional saddle-point stagnation flows may be negative, but here the displacement thicknesses are positive for all values of ρ and μ. Both displacement thicknesses vanish at $\rho = 1$, as noted in §3, and the lower fluid's thickness parameter A_1 tends to zero as $\mu_1 \to \infty$. For this latter limit, the lower fluid begins to behave as a solid impermeable wall, and the flow then resembles oblique stagnation-point flow over a rigid plate. Indeed, we find $A_2 \to 0.6479$ as $\mu_1 \to \infty$, in agreement with (Dorrepaal, 1985) for stagnation-point flow of a homogeneous fluid impinging on a flat plate. Figure 4 gives the scaled interfacial velocities $f'(0)/\sin\alpha_2$ and $g'(0)/\cos\alpha_2$ for different density and viscosity ratios. Both velocity components tend to zero as the density of the upper fluid vanishes.

From equation $(20)_2$ it is apparent that once the quantities $K_i \cos\alpha_i$ are nonzero, a specific relation between α_1 and α_2 must exist in order for the interface to remain flat: namely, for each value of $\rho \neq 1$ and $0 < \alpha_2 < \pi/2$ there is a unique value of α_1 lying in the range $\pi/2 < \alpha_1 < \pi$. Furthermore, the relation $(20)_1$ specifies a particular strain-rate ratio β. Figure 5 shows the solution for an air-water system, with the corresponding horizontal velocity components at $x = 0$, $x = \pm 50$ and $x = \pm 150$ displayed below the streamline field. Note that the lower fluid in the $x = -150$ profile has a minimum at $z \approx -3.18$. The flow in each fluid layer asymptotically approaches the respective rotational oblique far-field streamline flows as $|z| \to \infty$, and the intensity of the horizontal motion increases linearly with $|x| - x_0$. Figure 5 shows the variation of θ_1 as a function of θ_2 for three different two-fluid systems, *viz.* air/water, water/mercury, and olive oil/water. For $\rho > 1$ one obtains solutions $\theta_1 > \theta_2 + \pi/2$, with near equality for the olive oil/water system.

5. Discussion

We have considered the interaction between two planar oblique stagnation-point flows of different immiscible fluids, each occupying a half-plane of infinite horizontal extent normal to gravity. Only oblique flows that

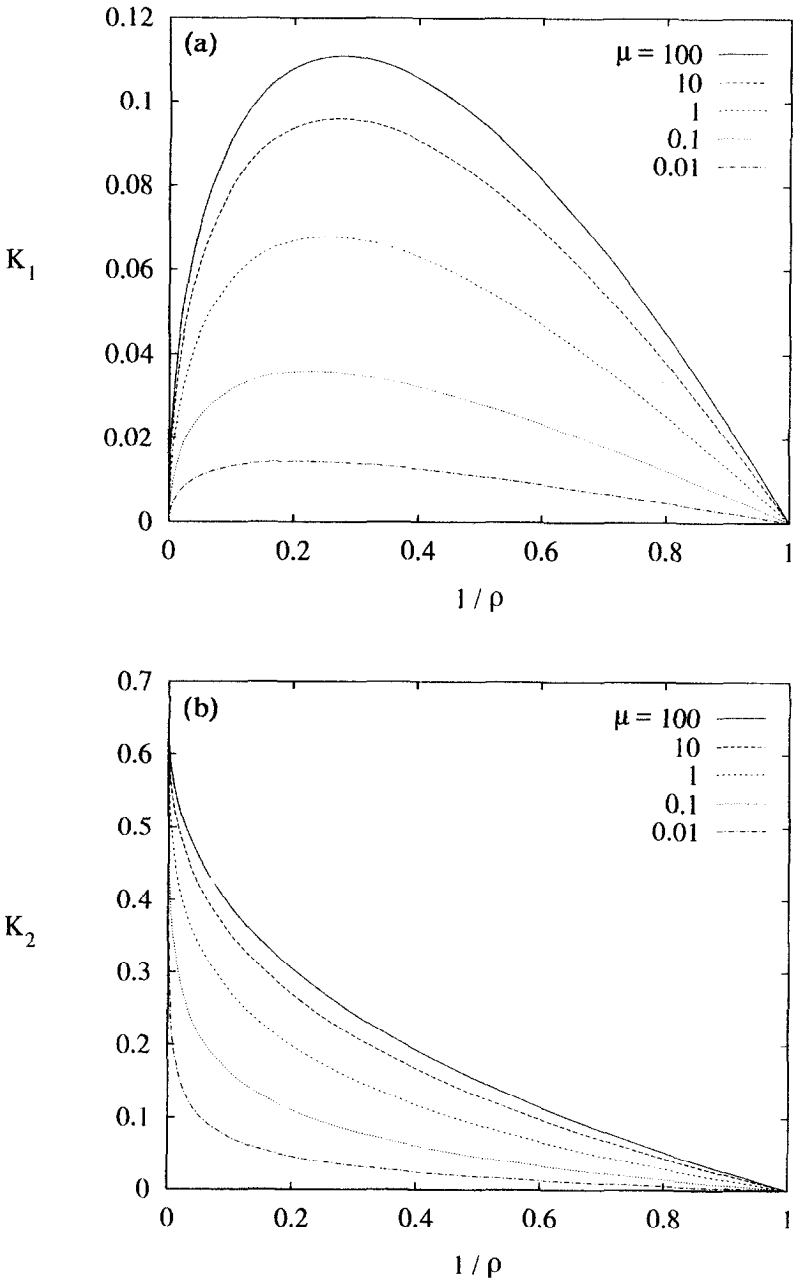

Fig. 3. – Displacement thickness parameters K_1 and K_2 as a function of the inverse density ratio for selected values of the viscosity ratio. One sees that the displacement thickness in each fluid is positive and that K_1 is not a monotonic function of the density ratio.

possess a flat interface have been studied. For equal density fluids a variety of impinging oblique stagnation flows exists, the sole requirement being that the Hiemenz component of the flow in each fluid have identical strain rates, *viz.* $\beta \sin \alpha_1 = \sin \alpha_2$. In this case, the uniform shear components can be either co-current or counter-current. When the densities are not equal, on the other hand, the interfacial normal stress in each fluid depends on both the displacement thickness of the Hiemenz flow component and the strain rate of the uniform

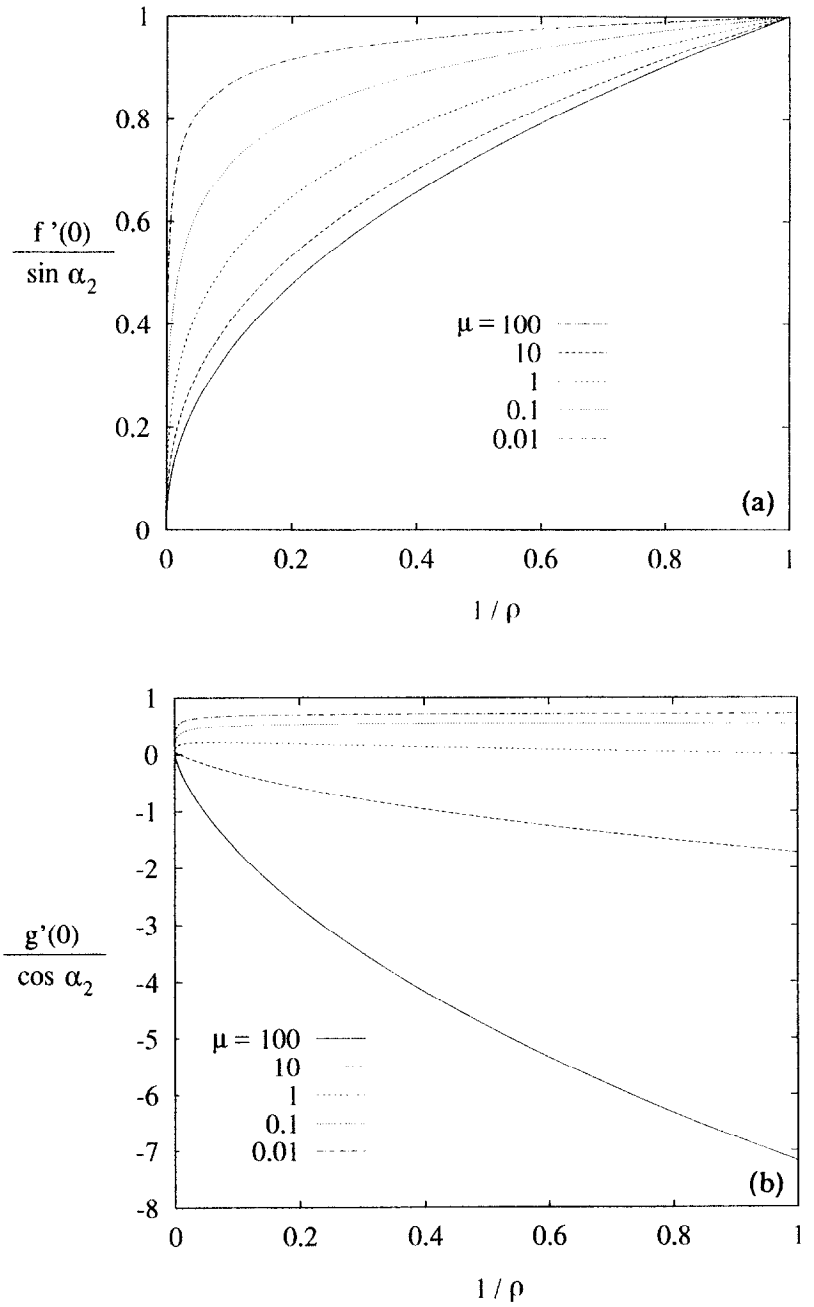

Fig. 4. – Hiemenz and shear-flow components of the intefacial velocity as a function of $1/\rho$ at selected values of μ.

shear component; in this case the uniform shear components $g'(z)$ form a unique counter-current flow at each value of θ_2 for a given pair of immiscible fluids.

The explicit exact solutions found for $\rho = 1$ are special in the sense that for prescribed values of ρ, μ, and $0 < \theta_2 < \pi/2$, there is an infinity of solutions $0 < \theta_1 < \pi$ in the lower fluid. Equation $(40)_2$ shows that the shift of the stagnation point from the origin has the same functional dependence on α_2 as that found by (Dorrepaal, 1985) for oblique stagnation-point flow impinging against a flat wall; however for the case most closely resembling his, that of the symmetric impingement of identical fluids obtained when $\mu = R = 1$,

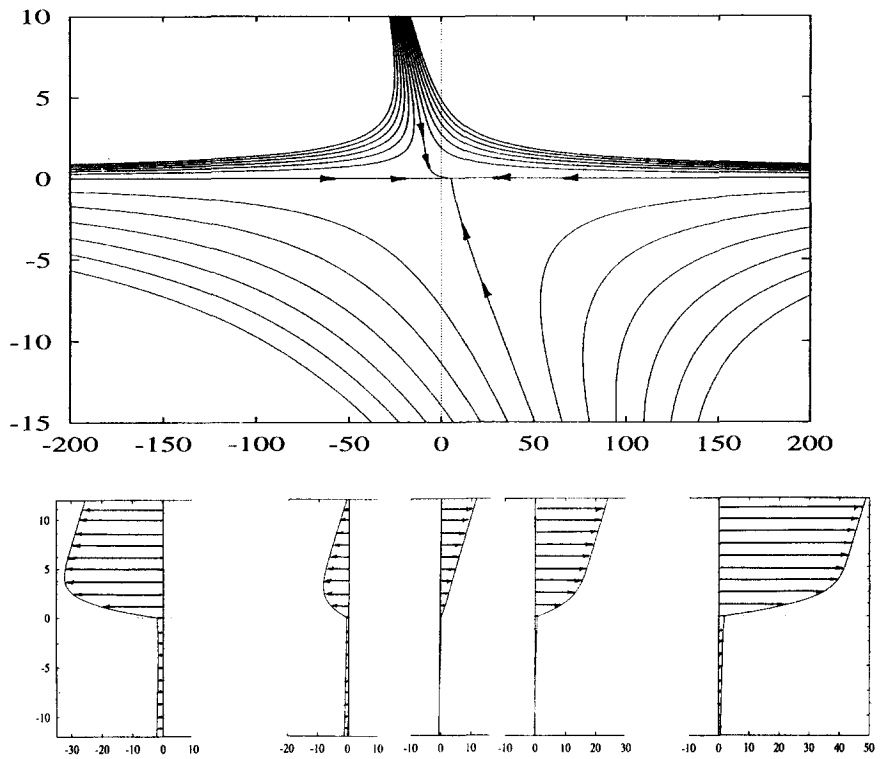

Fig. 5. – Streamline pattern for an air-water system for $\mu = 64$, $\rho = 815$, $\theta_2 = 72.2^o$. The lower fluid solution response gives $\theta_1 = 119.75^o$ and $\beta = 0.027$. Horizontal velocity profiles at $x = 0$, $x = \pm 50$ and $x = \pm 150$ are displayed below the streamline field.

the shift x_0 is smaller since the multiplicative constant in equation $(40)_2$ is $k = -\sqrt{2/\pi} \doteq -0.798$, whilst (Dorrepaal, 1985) found $k \doteq -1.411$.

One can readily generalize the present results to include the effect of buoyancy across an inclined interface. Taking a coordinate system $(\tilde{x}, \tilde{z})$ tangential and normal to the interface inclined at angle ϕ with respect to the horizontal, the balance in normal stress at the interface yields, to within a constant pressure, the conditions

$$G\,(\rho - 1)\sin\phi - [\beta K_1 \cos\tilde{\alpha_1} + K_2 \cos\tilde{\alpha_2}] = 0, \qquad \beta = \frac{1}{\sqrt{\rho}} \frac{\sin\tilde{\alpha_2}}{\sin\tilde{\alpha_1}},$$

where $\tilde{\alpha_1}$ and $\tilde{\alpha_2}$ correspond to the parameterization (7) with θ_i replaced by $\tilde{\theta_i} + (-1)^i\phi$, and $G = g/\sqrt{\nu_2\beta_2^3}$ is the appropriately normalized gravity. The first relation determines a unique interface tilt angle ϕ necessarily lying between a given pair of far-field angles θ_i. This relation is implicit since the $\tilde{\alpha_i}$ depend on ϕ. Note also the obvious result that buoyancy effects for an inclined interface vanish when $\rho = 1$.

One may also consider the problem of finding the response of a quiescient lower fluid to an imposed oblique stagnation-point flow of the upper fluid, as did (Wang, 1985) for the special case of normal stagnation-point flow. In Wang's problem, however, the interfacial normal-stress condition at the flat interface is only approximately satisfied either by considering small values of β or by restricting the analysis to a region local to the stagnation point. The same holds true when the upper fluid is an oblique stagnation-point flow, and one would solve the modified form of equations $(23)_1$ and $(24)_2$

$$F_1''' + F_1F_1'' - (F_1')^2 = 0, \qquad H_1'' + F_1H_1' - F_1'H_1 = 0,$$

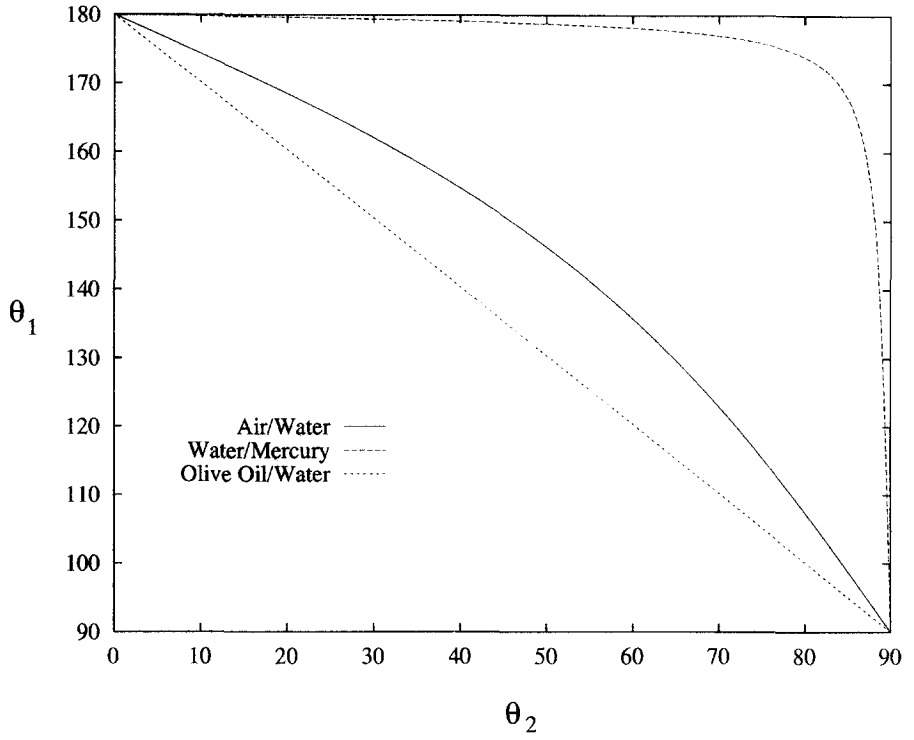

Fig. 6. – Compatible asymptotic streamline angles θ_1 plotted as a function of asymptotic driving streamline angles θ_2 for three different two-fluid systems.

with the original interfacial conditions, except that the far-field conditions become $F_1'(\infty) = H_1'(\infty) = 0$. In order to satisfy the normal-stress boundary condition *exactly*, one would have to allow for a spatially deformed interface. A linearized study of interfacial deformation for an inviscid two-fluid stagnation-point flow has been reported by (Erickson and Olfe, 1978). The viscous interfacial deformation is also of interest, and is currently part of our work in this area.

Consideration must be given to the stability of these exact solutions to the Navier-Stokes equations. Self-similar disturbances for plane stagnation-point flow on a solid plate are known to be linearly stable (Lyell and Huerre, 1985; Brattkus and Davis, 1991), but the presence of the interface allows for the possibility of a spatial-temporal instability. A Reynolds number Re_x based on the distance $x - x_0$ from the stagnation point can be introduced to perform the stability analysis for positive and negative values of Re_x. We speculate that the neutral stability boundaries will be, in principle, qualitatively similar to those found by (Coward and Hall, 1996) for uniform blowing of one (finite depth) fluid against an oncoming Hiemenz stagnation-point flow. In the present problem competing instability mechanisms will come into play at different values of α_i. For example, at low values of α_i when the flow is predominantly a discontinuous shear flow across the interface, the motion will be unstable to viscosity and/or density stratification across the interface as in the work of (Hooper and Boyd, 1983). An excellent review of such instability mechanisms in two-fluid systems is given in (Joseph and Renardy, 1993).

Acknowledgements. – The authors are indebted to Patrick Huerre and the other light-hearted members of LadHyX for their wonderful hospitality during our stay at École Polytechnique. We are indebted to Buck Danny for sharing his insight into the effects of oblique stagnation-point flow on swept-wing aircraft during practice

combat manuvers. BST is grateful for the support of a NSF-NATO Postdoctoral Research Fellowship, and PDW is grateful to École Polytechnique for six months support as Maître de Researche.

REFERENCES

BRATTKUS K., DAVIS S. H., 1991, The linear stability of plane stagnation-point flow against general disturbances, *Quart. J. Mech. Appl. Math.*, **44**, 135-146.

BURDÉ G. I., 1995, The construction of special explicit solutions of the boundary-layer equations. Unsteady flows, *Quart. J. Mech. Appl. Math.*, **48**, 611-633.

COWARD A. V., HALL P., 1996, The stability of two-phase flow over a swept wing, *J. Fluid Mech.*, **329**, 247-273.

DAVEY A., 1960, Boundary-layer flow at a saddle point of attatchment, *J. Fluid Mech.*, **10**, 593-610.

DORREPAAL J. M., 1986, An exact solution of the Navier-Stokes equation which describes non-orthogonal stagnation-point flow in two dimensions, *J. Fluid Mech.*, **163**, 141-147.

ERICKSON G. G., OLFE D. B., 1978, Growth and decay of perturbations at an interface in a stagnation counterflow, *J. Fluid Mech.*, **84**, 401-410.

HADAMARD J., 1911, Mouvement permanent lent d'une sphére liquide et visqueuse dans un liquide visqueux. *Comptes Rendus*, **152**, 1735.

HIEMENZ K., 1911, Die Grenzschicht an einem in den gleichförmingen Flussigkeitsstrom eingetauchten geraden Kreiszylinder. *Dinglers Poly. J.*, **326**, 321-410.

HOMANN F., 1936, Der Einfluss grosser Zähigkeit bei der Strömung um den Zylinder und um die Kugel. *ZAMM*, **16**, 153-164.

HOOPER A. P. W. BOYD G. C., 1983, Shear flow instability at the interface between two viscous fluids. *J. Fluid Mech.*, **128**, 507-528.

HOWARTH L., 1951, The boundary layer in three dimensional flow. Part II. The flow near a stagnation point. *Phil. Mag.* Series 7, **42**, 1433-1440.

JOSEPH D. D., RENARDY Y. Y., 1993, *Fundamentals of Two-Fluid Dynamics*, Vols. 1 & 2. Springer.

LYELL M. J., HUERRE P., 1985, Linear and nonlinear stability of plane stagnation flow, *J. Fluid Mech.*, **161**, 295-312.

PRESS W. H., FLANNERY B. P., TEUKOLSKY S. A., VETTERLING W. T., 1992, *Numerical Recipes*, 2*nd* edition, Cambridge University Press, p. 963.

ROSENHEAD L. (Editor) 1963, *Laminar Boundary Layers*, Oxford University Press, 688 p.

STUART J. T., 1959, The viscous flow near a stagnation point when the external flow has uniform vorticity, Reader's Forum, *J. Aero/Space Sci.*, **26**, 124-125.

TAMADA K., 1979, Two-dimensional stagnation-point flow impinging obliquely on a plane wall, *J. Phys. Soc. Japan*, **46**, 310-311.

WANG C. Y., 1974, Axisymmetric stagnation flow on a cylinder, *Quart. Appl. Math.*, **32**, 207-213.

WANG C. Y., 1985, Stagnation flow on the surface of a quiescent fluid – An exact solution of the Navier-Stokes equations, *Q. Appl. Math.*, **43**, 215-223.

WANG C. Y., 1992, The boundary layers due to shear flow over a still fluid, *Phys. Fluids A*, **4**, 1304-1306.

(Manuscript received April 25, 1997;
Revised and accepted December 18, 1997.)